Regional Studies in Marine Science 95 (2026) 104858

Contents lists available at ScienceDirect

Regional Studies in Marine Science

journal homepage: www.elsevier.com/locate/rsma

Spatio-temporal changes of Chlorophyll-a over the Eastern Mediterranean: Investigation of shipping, wildfires and dust events

Muhittin Gunes Onay [a], Serra Saracoglu [a,b], Elif Pehlivanoglu [a], Burcak Kaynak [a,*]

[a] School of Civil Engineering, Department of Environmental Engineering, Istanbul Technical University, Istanbul, Türkiye
[b] School of Engineering, Department of Environmental Engineering, Gebze Technical University, Kocaeli, Türkiye

ARTICLE INFO

Keywords:
Chl-a
Dust
Eastern Mediterranean
Livestock carrier
Shipping
Wildfires

ABSTRACT

This study examines the effect of maritime activity, wildfires, and dust storms on phytoplankton growth and presents a comprehensive five-year spatio-temporal assessment of Chl-a levels across the study area covering the Sea of Marmara, the Aegean Sea, and the Eastern Mediterranean, including coastal and open sea areas. Investigations utilizing GCOM retrievals revealed areas and intervals of increased Chl-a levels. A novel quantitative method was developed to categorize open sea areas based on shipping intensity, demonstrating a significant association between high shipping activity and elevated Chl-a concentrations for the first time in the literature. The association was particularly remarkable during times of limited phytoplankton growth in the Eastern Mediterranean. In addition, three specific episodes focusing on one anthropogenic (shipping-livestock) and two natural sources (wildfire and dust) were selected for the investigation of high Chl-a concentrations in open sea. Dust episode exhibited the most widespread and intense Chl-a increase, followed by wildfire episode with lower Chl-a increase. On the other hand, livestock episode indicated more localized, but intense increases. These natural and anthropogenic factors elevated Chl-a levels compared to pre- and post-event periods. These findings underlined the crucial role of overlooked shipping activities on phytoplankton dynamics in open seas. Natural events such as wildfires and dust storms are anticipated to occur more frequently and severely in the Mediterranean due to climate change, highlighting the need for efforts to quantify and mitigate shipping activities that might contribute to algal blooms.

1. Introduction

The growth of phytoplankton, the base of oceanic food webs, is primarily regulated by the availability of nutrients and light, and phytoplankton respond rapidly to changes in environmental conditions (Kotta and Kitsiou, 2019a). The growth rate of phytoplankton may differ depending on their location and is higher in coastal areas such as estuaries and bays with terrestrial nutrient inputs or nutrient loading from ships due to limited water exchange (Wang et al., 2024). On the other hand, in the open sea, the nutrients might be transported via air through dust storms, volcanoes and wild fires (Hamilton et al., 2025) to support phytoplankton growth.

Chl-a is widely used to evaluate phytoplankton abundance and ecosystem health (Chen et al., 2024) and it is one of the key optical properties that define eutrophication status of aquatic ecosystems along with Total Suspended Matter (TSM). TSM consists of insoluble inorganic and organic particles, such as clays, sediments, algae, and other aquatic microorganisms (He et al., 2013) and it is an essential parameter for assessing water color in environmental remote sensing (Sun et al., 2024). A significant linear relationship exists between Chl-a and TSM, as determined from both in-situ measurements and satellite retrievals (Maslukah et al., 2022). Further, Chl-a concentrations are key indicators for forecasting ocean net primary productivity, which is essential for marine ecosystem management (Xu et al., 2023).

Remote sensing data from several satellites have been utilized in the literature to assess Chl-a concentrations using different instruments such as MODIS (El Hourany et al. (2017) or through multi-satellite observations (SeaWiFS, MODIS-Aqua, MERIS, and VIIRS sensors) (Kotta and Kitsiou, 2019a; Salgado-Hernanz et al., 2019). In the Eastern Mediterranean, seasonal variations were generally marked by a phytoplankton growth period starting in late fall/winter extending to spring (El Hourany et al., 2017; Kotta and Kitsiou, 2019a; Kournopoulou et al., 2024), lasting an average of 150 days (Salgado-Hernanz et al., 2019). In contrast, the period from May to October corresponds to a low-growth

* Correspondence to: Department of Environmental Engineering, Istanbul Technical University, Maslak, Istanbul 34469, Türkiye
E-mail address: kaynakbu@itu.edu.tr (B. Kaynak).

https://doi.org/10.1016/j.rsma.2026.104858
Received 8 July 2025; Received in revised form 14 February 2026; Accepted 16 February 2026
Available online 19 February 2026

phase.

The rate at which Chl-a concentration decreases with the distance from the coast varies depending on local environmental conditions, river outflows, and anthropogenic activities. A general decreasing trend with distance from the shore is observed; however, generally the depth of the water instead of the distance from the coast is used to distinguish coastal areas and open sea in terms of bloom patterns of Chl-a (Kim et al., 2024). Nearshore areas were defined up to 50 m depth in the Eastern Yellow Sea (Kim et al., 2024; Son et al., 2005; Xuan et al., 2011), whereas studies in the Mediterranean have considered nearshore areas to extend to depths up to 200 meters (El Hourany et al., 2017; Salgado-Hernanz et al., 2019).

Measurements of Chl-a can be used to study both anthropogenic and natural airborne pollution effects on Chl-a concentrations. One of the anthropogenic effects is the shipping industry (Gössling et al., 2021) and marine environment is polluted by ships in different ways (i.e., air, water, and noise pollution) (Bilgin Güney and Kinaci, 2024; Viana et al., 2014; Yu et al., 2025). Shipping sector has significant amount of air pollutants released into the atmosphere due to their intensive fossil fuel use of their engines (Aulinger et al., 2016; Raut et al., 2022; Wang et al., 2025). Along with other pollutants, they emit nitrogen oxides, which can be deposited onto the ocean as nitrate and other nitrogen compounds through wet and dry deposition (Chen et al., 2020). Nitrogen is a critical nutrient for phytoplankton growth, particularly in nutrient-limited regions (Browning and Moore, 2023) in open seas far away from the coastlines. Increased nitrogen deposition from shipping can act as a nutrient, enhancing phytoplankton productivity. In addition, ships take in and release ballast water, which can introduce nutrients (Gaballa Altohame Jalgaif et al., 2019) into the sea, potentially leading to eutrophication (Raudsepp et al., 2019). Another possible pathway of ship-based pollution into the seas is the discharge of wastewater (Shu et al., 2022). Wastewater from domestic use in ships such as showers and kitchens often contain detergents, food residues and other organic matter that decompose and release nutrients (Chen et al., 2022) in addition to high concentrations of nitrogen and phosphorus mainly from human waste (Lappalainen et al., 2024). Raudsepp et al. (2019) investigated ship-based nutrient dynamics and effect on eutrophication in Baltic Sea, and calculated nutrients from shipping emissions and ship-based wastewater. Ship-based N deposition was estimated to contribute up to 10 % increase in Chl-a concentration. Zhang et al. (2021) investigated impact of shipping emissions on phytoplankton growth over the Northwest Pacific Ocean, and predicted a contribution up to 8 % increase in Chl-a concentration due to ship-based N deposition.

When specific types of marine vessels are considered, livestock carriers are among the significant sources of pollution. These livestock carriers are usually old cargo vessels converted to transport live animals (e.g., sheep, cattle and goats), with an average fleet age of 43 (Bossard and Bonnemains, 2024). 75 % of the livestock carrier vessels investigated between 2021 and 2023 were lacking proper pollution prevention techniques (Bossard and Bonnemains, 2024) possibly discharging high levels of nutrients due to the livestock waste (manure and urine) (Princewill et al., 2012).

In addition to anthropogenic sources, there are natural sources of nitrogen and other nutrients such as wildfires and dust transport. Most wildfire research has focused on terrestrial ecologies (Kala, 2023; Martin et al., 2016) and relatively little is known about the effects of wildfires on marine environments, despite the fact that many wildfires occur in coastal areas (Eke et al., 2024; Giannaros et al., 2022). As wildfire frequency and intensity continue to rise globally, understanding their impacts on ocean ecosystems is becoming increasingly important. Wildfire emissions and ash are rich in nitrogen, phosphate, iron, and silicate and a positive correlation has been observed between wildfires and phytoplankton production in ocean waters in Kimberly coast, Australia (Liu et al., 2022). Recent studies have shown that wildfire ash can act as a fertilizer for surface ocean waters often leading to bloom conditions (Kramer et al., 2020; Nguyen et al., 2024). Similarly, wildfires near lakes have been associated with increased phytoplankton community composition during and after fire events (Charette and Prepas, 2003). Similarly, dust storms transport essential nutrients to nutrient-limited regions like the open ocean (Nguyen et al., 2024) and promote phytoplankton growth (Bigio et al., 2020; Meng et al., 2023).

The main aim of this study is to estimate the spatio-temporal variation of Chl-a and TSM levels in the Sea of Marmara, Aegean Sea and the Eastern Mediterranean, with a focus on coastal regions of Türkiye for the years of 2019–2023. Chl-a and TSM levels were investigated in selected coastal areas, on important shipping routes, and in open sea regions. There is no comprehensive study about the spatio-temporal changes of Chl-a with high resolution GCOM (Global Change Observation Mission) instrument focusing on these regions affected by different anthropogenic and natural nutrient sources. Thus, the impact of shipping, wildfires, and dust transport on phytoplankton growth was investigated via high-resolution GCOM Chl-a retrievals.

2. Methodology

.1. Study area and time-interval

The study area covers Sea of Marmara, Aegean Sea and the Eastern Mediterranean (Fig. 1) for coastal analysis, whereas Aegean Sea and the Eastern Mediterranean were focused in open sea and episodic analysis. The Mediterranean is one of the nutrient-poor marine areas in the world (Oms et al., 2024). While in-situ measurements across the Eastern Mediterranean remain limited, remote sensing measurements via satellites provide increasing spatial resolution data.

Due to the significant impact of terrestrial sources, the study area was categorized into two overall regions: *coastal* and *open sea*, and these regions were investigated separately. The coastal zone was defined as the area from the shoreline up to 200 m depth, while the open sea began beyond this 200 m depth boundary (El Hourany et al., 2017; Salgado-Hernanz et al., 2019). Bathymetry data were obtained from the EMODnet Bathymetry portal (EMODnet, 2025a). In addition to investigating the overall region, several sub-areas were selected for the study: 14 *coastal* and 10 *open sea* areas for detailed investigation (Fig. 1). Open seas were selected as four areas with higher Chl-a levels and main shipping routes passing, and six areas with limited shipping density. In particular, S01 was selected off the coast of Antalya, and S02 was in the Rhodes Gyre region, situated south of Rhodes Island and east of Crete Island. S03 lies along the shipping routes connected to the Suez Canal, and S04 is also positioned along the Suez Canal route, located between Africa and Europe. A total of 14 *coastal regions* selected for further investigation are Izmit (C01), Gemlik (C02), Saros (C03), Edremit (C04), Aliaga (C05), Izmir (C06), B. Menderes (C07), Gulluk (C08), Gokova (C09), Fethiye (C10), Antalya (C11), Tasucu (C12), Mersin (C13), and Iskenderun (C14) (Fig. 1 and Table 1).

The time-interval investigated was the five-year period of 2019–2023. In addition, specific episodes of 11–12 days were selected to investigate important anthropogenic and natural impacts in the open sea areas (Table 2). The episodes were investigated with pre- and post- intervals and the enhancements during the episodes were estimated.

.2. Ship route density

Route density (RD) data by the European Maritime Safety Agency (EMSA) were obtained from European Marine Observation and Data Network (EMODnet, 2025b) with a spatial resolution of 1×1 km^2. It provides annual, seasonal, and monthly route density data (#routes/km^2/month) for different vessel types, including cargo, tanker, fishing, passenger, and other, as well as total vessel traffic. Since cargo and tanker ships account for approximately 80 % of total emissions in the Mediterranean (Pseftogkas et al., 2021), their monthly route density data were specifically included in the analysis, in addition to total

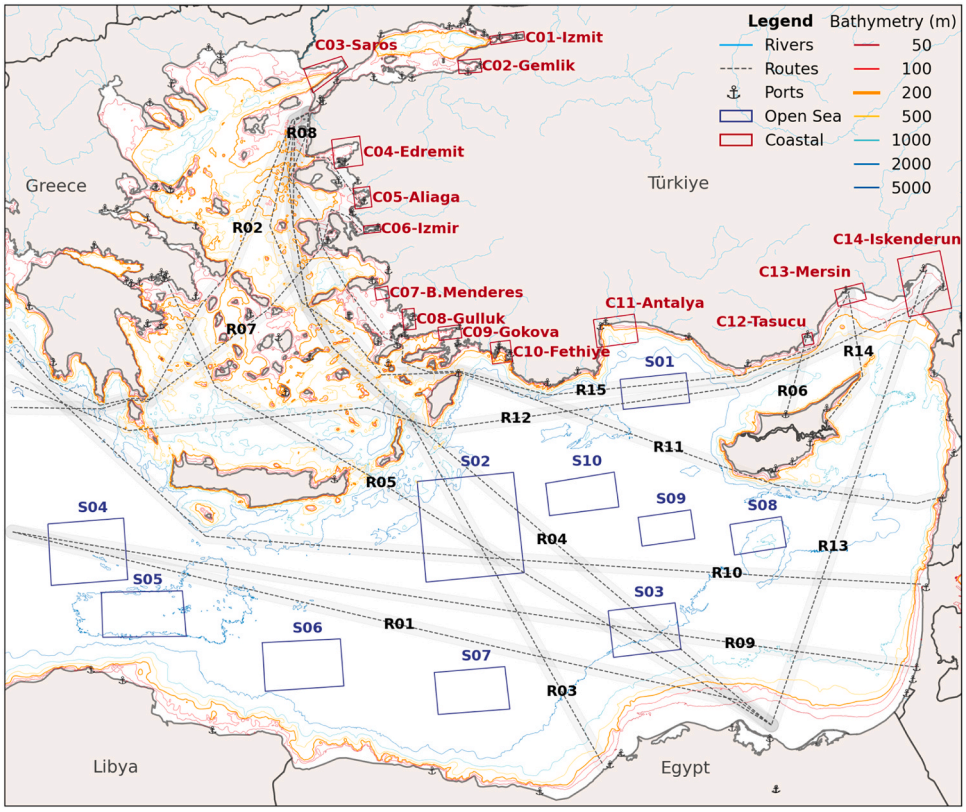

Fig. 1. The study area with focused sub-regions, routes, ports, major rivers, and bathymetry.

vessels for the selection of main routes with busy shipping traffic (Figure S1, Table 1).

Surface currents' speed varies depending on environmental conditions in the Eastern Mediterranean. Average current speed ranging between 10 cm/s (Amitai et al., 2010), 19 cm/s (Poulain et al., 2012) and 80 cm/s (Gucel and Sakalli, 2024). In this study, 30 cm/s (=1.08 km/h) average current speed was used. Phytoplankton doubling time is approximately 8 h (Freilich et al., 2022) and combining this two information the width of the routes was defined as 20 km with 10 km from the route centerline to each direction. To avoid impacts of land-based nutrient sources and transport of nutrients by upwelling and sinking processes, Chl-a and TSM concentrations for each route were calculated only in open sea regions with depths more than 200 m. In addition to the selected routes, another, more quantitative, approach was applied to investigate and quantify the impact of shipping on Chl-a levels. A more precise quantification of RD was done by estimating the percentile of every 1 × 1 km^2 grid for each year using the annual total RD for the study area. These percentiles were then used to categorize Chl-a concentrations according to the intensity of the shipping for the grids. In that selection, the coastal grids within 200 m bathymetry were excluded from the analysis to eliminate the impact of terrestrial sources.

.3. *Satellite retrievals*

GCOM-C Chl-a product algorithm is based on the standard blue-green band ratio (OCx) algorithm (O'Reilly et al., 2000) and the Color Index approach (Hu et al., 2012) with coefficients derived from the NASA NOMAD bio-optical dataset and further adjusted for the SGLI spectral bands. Additional in-situ observations collected around Japan supported evaluation and improvement of the retrieval performance. TSM algorithm is an empirical multiple regression model that combines the reflectance ratio Rrs(443)/Rrs(565) which represents organic suspended matter, with the single-band reflectance Rrs(565), which represents inorganic suspended matter, to estimate total suspended matter concentrations (Toratani, 2021). Validation of these products were performed during the period 2018–2021 by comparing SGLI retrievals with in-situ measurements (ship observations, MOBY, BOUSSOLE, AERONET-OC), using temporal (±3 h) and spatial (5 ×5 pixel) collocation criteria. These analyses showed that version 3 product meets the standard accuracy requirements (-60 % to +150 %) (-59–141 % for Chl-a and −59–145 % for TSM) with improved valid pixel coverage in coastal and sunglint regions (JAXA, 2022).

In this study, 250-meter daily scene-based resolution Level 2 (L2) in-water properties (IWPRQ) products (Major version 3, full version 3000), Chl-a (CHLA, in units of mg/m^3) and total suspended matter (TSM, in units of g/m^3) with an equator-crossing time of 10:30 (am) were obtained from G-Portal in April 2025 (G-PORTAL, 2025a). L2 products were converted to GeoTIFF format using the SGLI Map Projection & GeoTIFF Conversion Tool (Ver. 1.2) provided by JAXA (G-PORTAL, 2025b). To convert GeoTIFF digital numbers (DN) to physical quantities, geophysical conversion coefficients (slope/offset) were applied using product-specific values (CHLA: slope = 0.0016, offset = 0.0; TSM: slope = 0.001, offset = 0.0), following the equation: DN × slope + offset. To conduct a uniform spatial and temporal assessment over the Eastern Mediterranean, then pixel center points were processed with 1 × 1 km^2 EMOD grids to estimate daily, moving 7-day and 14-day, monthly and selected period averages for the years of 2019–2023.

The GCOM-C version 3 validation results between retrievals and field observations showed that Chl-a and TSM products achieved standard accuracy of −59 to + 141 % and −59 to + 145 %, respectively (JAXA, 2022). Salem et al. (2025) compared GCOM Chl-a retrievals with in-situ measurements in Japan and East Asia between January 2018 and December 2023. In situ measurements indicated that GCOM (G-Portal) provides better agreement for Chl-a concentrations below 5 mg/m^3. In another study (Luang-on et al., 2024), GCOM accurately identified red tides in Gulf of Thailand confirming the GCOM reliability with in situ data (Salem et al., 2025).

Period selections were performed utilizing five-year monthly

Table 1
Selected sub-regions of coastal and open sea areas, and major routes in the study area.

Type	ID-SEA	Regions
Coastal	C01-MAR	Izmit
	C02-MAR	Gemlik
	C03-AEG	Saros
	C04-AEG	Edremit
	C05-AEG	Aliaga
	C06-AEG	Izmir
	C07-AEG	B. Menderes
	C08-AEG	Gulluk
	C09-AEG	Gokova
	C10-MED	Fethiye
	C11-MED	Antalya
	C12-MED	Tasucu
	C13-MED	Mersin
	C14-MED	Iskenderun
Open sea	S01-MED	South of Antalya
	S02-MED	Rhodes Gyre
	S03-MED	North of Egypt
	S04-MED	Southwest of Crete
	S05-MED	Southwest of Crete
	S06-MED	South of Crete - Northeast of Libya
	S07-MED	North of Egypt
	S08-MED	South of Cyprus
	S09-MED	Southwest of Cyprus
	S10-MED	West of Cyprus
Route	R01-MED	Mediterranean-Suez Canal
	R02-AEG	Mediterranean-Canakkale Strait
	R03-AEG	Alexandria-Canakkale Strait
	R04-AEG	Suez Canal-Canakkale Strait
	R05-AEG	Suez Canal-Pireus
	R06-MED	Tasucu-Kyrenia
	R07-AEG	Mediterranean-Izmir
	R08-AEG	Aliaga-Canakkale Strait
	R09-MED	Mediterranean-Ashdod
	R10-MED	Haifa-Mediterranean
	R11-AEG	Beirut-Canakkale Strait
	R12-MED	Mediterranean-Iskenderun
	R13-MED	Suez Canal-BOTAS
	R14-MED	Mersin-Famagusta
	R15-AEG	Mersin-Canakkale Strait

Table 2
Selected episodes with their pre- and post- time intervals.

Episode Type	ID	Region	Dates		
			Pre-	Episode	Post-
Livestock - Shipping	E01	MED	25 Jul–5 Aug 2023	6–17 Aug 2023	18–29 Aug 2023
Wildfire	E02	MED	18–27 Jul 2021	28 Jul–7 Aug 2021	8–17 Aug 2021
Dust	E03	MED	17–27 Mar 2022	28 Mar–7 Apr 2022	8–18 Apr 2022

analysis, and further investigated in-detail. The episodes were selected according to times of extreme Chl-a levels observed (dust), devastating-level natural hazards (wildfire), and investigating the local known environmental issues within study region and interval.

3. Results and discussion

The Mediterranean and the Sea of Marmara are very important in terms of international maritime traffic, and monthly route density distribution for all vessels between 2019 and 2023 varied spatially throughout the year (Figure S1). Istanbul and Canakkale Straits, Mersin, Iskenderun, Izmir, Piraeus, Alexandria, Haifa, Beirut and entrance of the Suez Canal had busy traffic and route density did not change for the whole year. Summer months showed slightly increased activity, especially in the Aegean Sea, likely due to seasonal ferry and cruise traffic. Winter months still maintained heavy traffic in the main shipping routes with predominantly cargo and tanker vessels. In 2023, maritime traffic increased compared to previous years. The Suez Canal had the passage of 18,880 vessels in 2019 and 18,830 vessels in 2020, but had increasing ship traffic with 20,694 vessels in 2021, and 23,851 vessels in 2022, and the canal achieved a new record with 26,434 vessels in 2023 (Suez Canal Authority, 2023). The major routes selected according to route density maps of 2019–2023 were given along with other selected regions (Table 1). Mediterranean-Canakkale Strait (R02) and Suez Canal-Canakkale Strait (R04) are the busiest routes in the study area. Maritime traffic along the Mediterranean-Suez Canal (R01) route increased over the years.

.4. Spatio-temporal variation of Chl-a

The evaluation of monthly Chl-a concentration distributions for the five years (2019–2023) over the Sea of Marmara, the Aegean Sea and the Eastern Mediterranean, indicated significant spatial and temporal variations. Chl-a concentrations were generally higher along the coast and near river outflows (Fig. 2). This increase was due to nutrient enrichment from agricultural runoff and wastewater discharge, which support phytoplankton growth (MoEUCC, 2022a). The monthly Chl-a distributions for five years indicated a decline in Chl-a concentrations, possibly due to the onset of water column stratification which limits nutrient availability in surface waters in summer months especially in open sea regions (Fig. 2 and Fig. 3). The study area consists of the Sea of Marmara in the north, the Aegean Sea and the Eastern Mediterranean in the south with different water quality and bathymetric characteristics (MoEUCC, 2022a, 2022b, 2022c). Being an inland sea with comparatively smaller area, the Sea of Marmara had the highest Chl-a concentrations. On the other hand, the Aegean Sea and the Mediterranean exhibited a difference between coastal and open sea regions (Figure S2). Open sea waters, especially in the Eastern Mediterranean, were oligotrophic, with monthly average Chl-a values dropping below 0.1 mg/m^3 in the summer months (Fig. 3). Coastal areas still showed higher concentrations, possibly due to terrestrial nutrient sources. Summer season appeared to have the lowest productivity. In fall months, Chl-a levels began to increase again, due to the breakdown of stratification, mixing of the water column, and renewed nutrient availability (Salgado-Hernanz et al., 2019; Kournopoulou, et al., 2024). Long term spatial and temporal TSM concentration distributions between 2019 and 2023 was similar with Chl-a (Fig. 3, Figure S3). TSM and Chl-a showed overlapping hotspots in open sea regions, since the main source of TSM is phytoplankton. However, coastal regions with intense industrialization and urbanization like coastal regions of Türkiye in the Aegean Sea might have different sources of TSM other than phytoplankton due to surface runoff and wastewater discharges resulting in different Chl-a and TSM patterns. Coastal Chl-a levels remained relatively stable, with slightly elevated concentrations during the winter months, likely due to increased nutrient inputs. A notable exception was observed between Jul-Sep 2021 (Figure S2c), when Chl-a levels increased in the Sea of Marmara and Aegean Sea, driven by impacts of the mucilage event (Balkıs Özdelice et al., 2023; Tuzcu Kokal et al., 2022). Chl-a levels in the Sea of Marmara and north of Aegean Sea were higher year-around with a slight decrease in summer season. However, Chl-a concentrations in the south Aegean Sea and the Mediterranean open sea typically displayed a clear seasonal pattern, with lower levels during summer, and a gradual increase starting in October, peaking in winter and early spring (Fig. 2 and Fig. 3) reflecting typical oligotrophic conditions of the Mediterranean open waters (Kournopoulou et al., 2024).

The problematic results of the Sea of Marmara having limited circulation and high coastal nutrient inputs were particularly observed during the 2021 mucilage crisis (Balkıs Özdelice et al., 2023; Demir, 2022). An increase in average SST from 16.1°C in 2015 to 17.6°C in 2021 (Tuzcu Kokal et al., 2022) was probably one of the reasons of the mucilage. When 2020 and 2021 Chl-a distributions are compared (Figure S2b and c), unexpectedly high concentrations were noticeable in

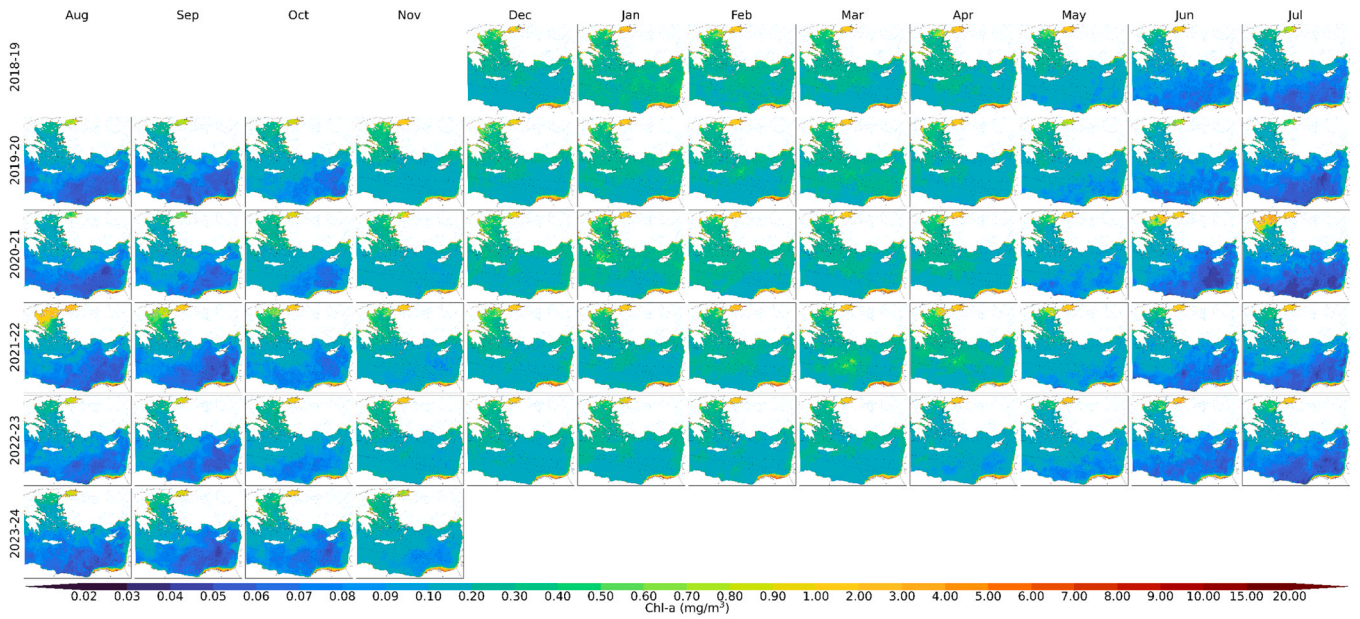

Fig. 2. Monthly average Chl-a distributions of the study area from Dec 2018 to Nov 2023.

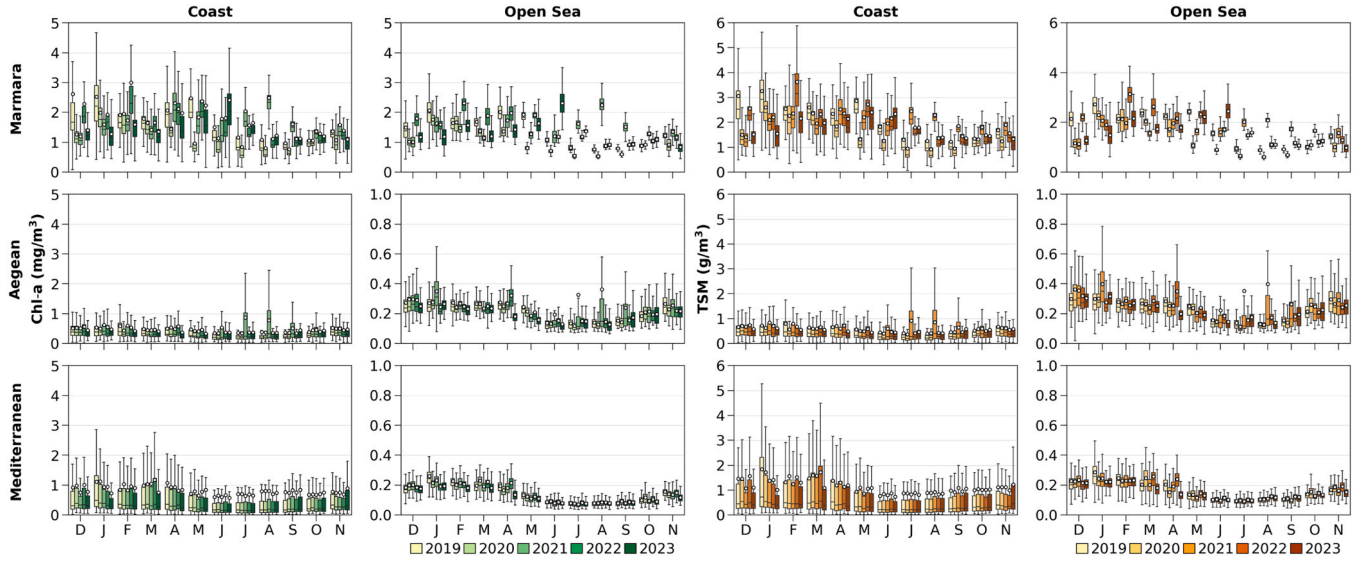

Fig. 3. Monthly average Chl-a and TSM distributions for the Sea of Marmara (top), Aegean Sea (center), and the Eastern Mediterranean (bottom) for five years (box: 25–75 percentiles (Q1-Q3; Interquartile range (IQR)), whiskers: Q1 - 1.5 ×IQR and Q3 + 1.5 ×IQR, central line: median, circle: mean).

spring and summer 2021 due to this problem. The mucilage event affected several areas, including the Gulf of Izmit, Gulf of Gemlik, Kapidag Peninsula, Prince Islands, and various other coastal regions (Fig. 1, Table 1). Notably, in June 2021, daily Chl-a concentrations peaked at 21.7 mg/m^3 in the Gulf of Gemlik and reached 27.4 mg/m^3 in the Gulf of Izmit, indicating intense algal activity linked to the mucilage event, although the monthly average Chl-a levels during summer and fall of other years were generally around 1–2 mg/m^3. This result of the Sea of Marmara coastal areas suggested that TSM in the Marmara region was influenced by several factors, notably agricultural runoff, urban wastewater and industrial discharges, which contribute significantly to elevated monthly average TSM concentrations, often exceeding 2 g/m^3 (Figure S3) with a maximum monthly average of 3.6 g/m^3 occurring in Feb 2022 (Fig. 3). The Sea of Marmara was eutrophic and turbid, likely due to its semi-enclosed geography, Black Sea outflow, river discharges, urban and agricultural runoff, and dense maritime traffic.

Islands and river discharges play a crucial role in shaping the spatial distribution of Chl-a. In the Aegean Sea, discharges of Evros (Meric), Struma and Axios (Vardar) rivers enhanced productivity due to terrestrial sources. River-influenced zones and exit of Canakkale Strait showed higher Chl-a at the northern parts of Aegean Sea (Fig. 2, Figure S2). The northern and coastal regions were biologically more productive compared to the oligotrophic southern and open Aegean waters. Variation was relatively low compared to the Sea of Marmara. Chl-a levels were moderate year-round, with slightly elevated levels in winter and spring (Fig. 3). The presence of numerous Aegean islands (e.g., Lesvos, Chios) introduces localized upwelling zones (Androulidakis et al., 2017; Mamoutos et al., 2017; Tükenmez and Altıok, 2022) and strong vertical mixing (Nishioka et al., 2021) fostering elevated Chl-a values in their vicinity (Figure S2). Particularly during winter and fall, localized Chl-a hotspots were observed near some of these islands. In summer 2021, Chl-a concentrations in the northern Aegean Sea were noticeably higher

compared to other summer periods (Fig. 3), with elevated levels particularly evident around the Evros River outflow (Figure S2c). This result suggests that nutrient-rich water discharged from the river likely influenced phytoplankton growth and impacted water quality in the northern Aegean Sea.

In the Eastern Mediterranean, Chl-a levels exhibited a clear seasonal pattern, with higher values from winter to spring (Dec-Apr) and a decline in summer in both coastal regions and open sea (Fig. 3). Open sea regions showed low Chl-a values while elevated concentrations appear near the coasts (Fig. 2). Chl-a levels drop to monthly averages around 0.02–0.05 mg/m^3, especially in open waters in summer due to low biological productivity. Open waters were oligotrophic because of stratification and weak vertical mixing while Chl-a concentrations were high around the southeastern coast of the Mediterranean, especially near the Nile Delta (Fig. 2). The Nile Delta discharges nutrient-rich freshwater into the southeastern Mediterranean. Urbanized coastal regions around Alexandria, Beirut, and Tel Aviv contribute with wastewater discharge and surface runoff, supplying nutrients. Southeast

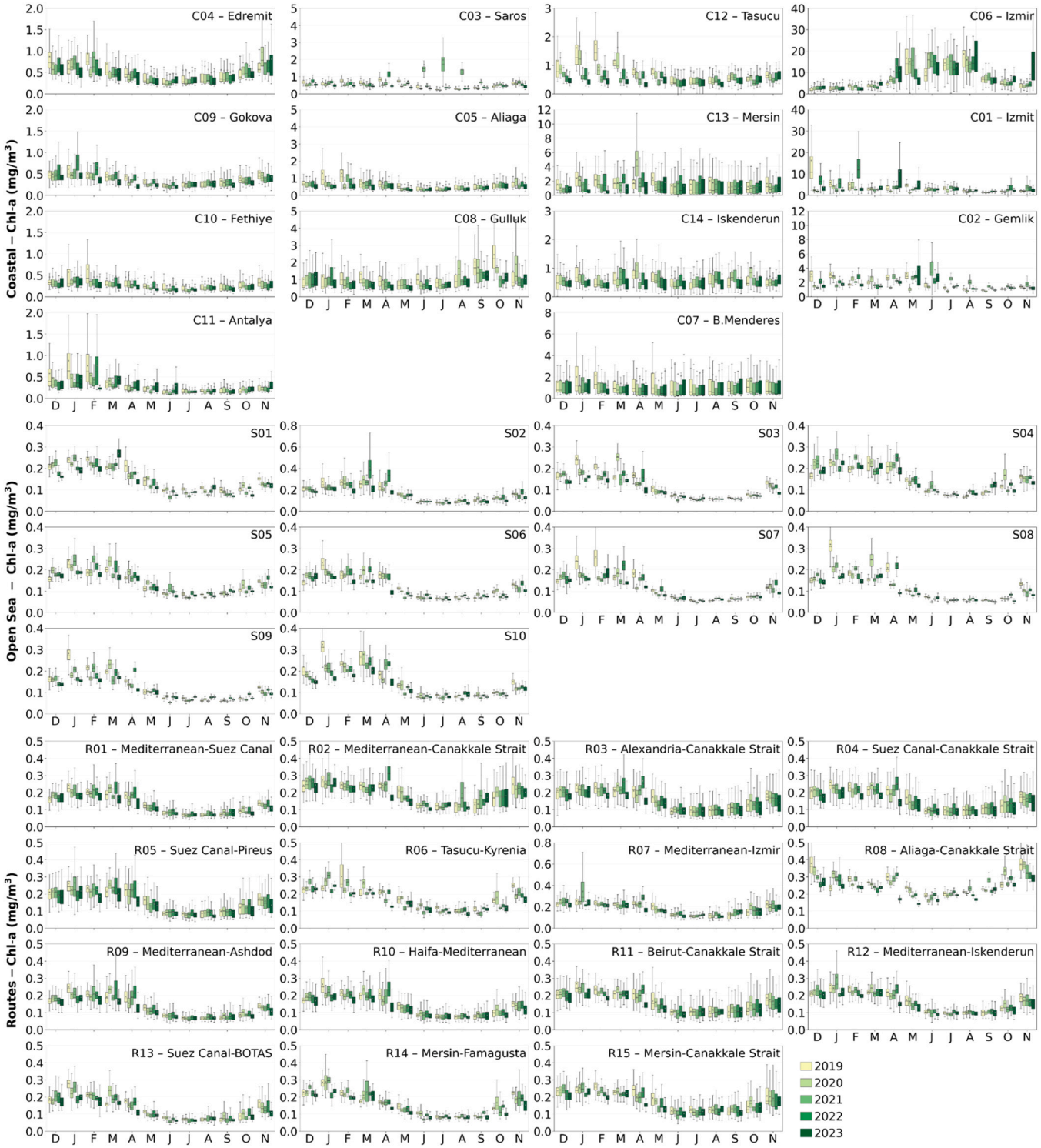

Fig. 4. Monthly average Chl-a concentrations for coastal (C01-C14) (top), open sea (S01–10) areas (center), and along the routes (R01-R15) (bottom) for five years.

depths are shallow compared to other Mediterranean coastal areas, which allow stronger vertical mixing and light penetration, supporting phytoplankton growth (Jäger et al., 2008). In the southeastern coast of the Mediterranean (especially around Nile Delta region), elevated Chl-a concentrations extend up to 60 km from the coast (Fig. 2). In the northern coast, Mersin region, high Chl-a levels were observed up to 25 km from the coast. In contrast, in the Eastern Mediterranean -specifically along the coasts of Syria, Lebanon, and Israel- as well as around Antalya and Fethiye of Türkiye, high Chl-a concentrations were limited within 5 km of the coast. This variation is influenced not only by the impact of land sources but also by regional differences in bathymetry, as Chl-a concentrations tend to decrease beyond the 200-meter depth contour, which occurs at varying distances from the coast in different areas (Fig. 1). Over the five-year period from 2019 to 2023, the coastal average Chl-a concentration were highest in the Marmara Sea, followed by the Aegean Sea with extreme levels in Jul-Aug 2021 and the lowest levels were observed in the Mediterranean (Fig. 3).

Due to Chl-a magnitude and variability in coastal regions, specific coastal areas with different conditions were investigated in detail (Table 1, Fig. 1). Selected 14 *coastal areas* can be divided into three categories according to their distinct Chl-a patterns (Fig. 4). Relatively clean bays such as Antalya, Edremit, Gokova, Fethiye, Saros along with slightly more polluted Aliaga and Gulluk exhibited high Chl-a concentrations in winter, and low concentrations in summer, consistent with typical Mediterranean seasonal trends previously reported in the literature (El Hourany et al., 2017; Kotta and Kitsiou, 2019a; Kournopoulou et al., 2024). In Saros, the mucilage event strongly affected the summer of 2021 (Jun-Sep). The Chl-a concentrations in the Gulf of Gulluk indicated an earlier rise starting in Aug different from other areas with maximum levels in late fall, not in winter in 2019–2020. The presence of numerous aquaculture farms in the Gulf of Gulluk may cause this anomaly (Bardakçı Şener and Tıraşın, 2024). In the recent years after 2020, reductions in Chl-a concentrations were observed possibly due efforts of coastal cleaning campaigns by municipalities of Mugla (Action Plan, 2020) covering the coastal areas of Gulluk (C08), Gokova (C09), Fethiye (C10). Aliaga (C05) region is a well-known industrial district with various pollution sources including industrial facilities, refineries and ship breaking which could also contribute to nutrient pollution.

Urbanized and industrialized regions like Izmir, Izmit, Gemlik showed elevated Chl-a levels without following the standard Mediterranean seasonal pattern. Monthly Chl-a distributions in Izmir had a unique profile with the highest levels occurring consistently reaching over 20 mg/m^3 suggesting a mix of extraordinary conditions supporting eutrophication in summer season. In the Gulf of Izmir, lower Chl-a levels were observed during the winter months, followed by a sharp increase starting in April, with peak concentrations between April and August (Fig. 4). This phytoplankton bloom is typical of eutrophic conditions in semi-enclosed coastal bays influenced by nutrient inputs from streams, urban runoff, and possible wastewater discharges. 7-day moving average Chl-a concentrations exceeded 30 mg/m^3 in summer of 2020 and 2021. The daily peak Chl-a in the Gulf of Izmir reached up to 75 mg/m^3 which is much higher than peak levels observed in the Amvrakikos Gulf (8 mg/m^3), a semi-enclosed, shallow basin affected by urban pollution (Kournopoulou et al., 2024). These levels indicated the importance of monitoring eutrophication risk and implementing effective nutrient management strategies in such regions. Unlike Chl-a, daily TSM levels did not show a sharp seasonal peak and remained relatively elevated year-round with maximum in summer, indicating persistent inputs of suspended particulate matter in to the Gulf of Izmir.

In Izmit and Gemlik in the Sea of Marmara, monthly average Chl-a concentrations reached up to 15 and 4 mg/m^3, with 7-day moving average concentrations of 10 and 2 mg/m^3, respectively. The highest monthly averages were not consistent with seasonality, but they were limited to single incidents with extreme values. Notably, the summer of 2021 showed increased Chl-a levels in Gemlik compared to other summer periods, likely due to the mucilage event. Chl-a concentrations were consistently higher in Izmit than Gemlik. Daily TSM indicating higher temporal variability than Chl-a in Gemlik than Izmit, suggesting presence of other suspended solids than phytoplankton in Gemlik.

As the last category, Iskenderun, Mersin, Tasucu, and B. Menderes Delta did not display the seasonal variations of the Mediterranean. Nevertheless, the range of variation in monthly Chl-a concentrations were larger. The daily Chl-a concentrations in the B. Menderes showed a base level around 1 mg/m^3 throughout the year with spikes above 5 mg/m^3 reaching up to 22 mg/m^3 in summer months of all years, especially in June and July which aligns with the agricultural practices for cotton farming. This summer spike was also evident in Mersin; however, the Chl-a levels were higher with moderate to high spikes occurring at other times as well with spikes above 3 mg/m^3 reaching up to 16 mg/m^3. The daily spikes observed in 2019 and 2020 were not observed in the following years and the levels were lower in Tasucu than Mersin and B. Menderes. In Iskenderun Bay, Chl-a concentrations were comparable with Tasucu without the higher levels observed in 2019 and 2020. The Chl-a concentrations remained relatively constant throughout the year, showing limited seasonal variability due to sustained nutrient inputs and the semi-enclosed structure of the bay (Fig. 2, Figure S2). The agricultural activities and large river discharges to Tasucu, Mersin, B. Menderes, industrial activities to Mersin, Iskenderun, and shipping activities with busy international ports in Mersin, Tasucu, Iskenderun likely contributed to increased nutrient input, influencing the local Chl-a concentrations (Fig. 4). Iskenderun, Mersin and Tasucu ports are the sole ports of Türkiye accepting livestock carriers with significant nutrient source via animal waste.

In addition to the overall assessment of open seas, ten specific open sea areas were selected: with high shipping route densities consisting of significant routes (S01-S04) and with more sparse route densities (S05-S10) (Fig. 1 and Fig. 5-left panel). Seasonal Chl-a variability in S01 was similar to general Mediterranean open sea trend (Fig. 4). In 2023, Chl-a concentrations were generally lower than in previous years, except for a peak observed in March. S02 was characterized by eddy circulation and nutrient upwelling due to Rhodes Gyre, which supports high primary productivity (Van Leeuwen et al., 2022) similar to the findings of Kournopoulou et al. (2024). As a result, Chl-a concentrations here were higher and showed a pronounced seasonal pattern compared to other open sea areas (Fig. 4). On the other hand, S03 had lower and S02 had higher Chl-a concentrations than the other areas selected as well as the Mediterranean overall with statistical significance (Mann–Whitney *U* test) (Figure S5). S04 displayed a typical seasonal pattern of oligotrophic open sea (Fig. 4). In S02 and S04, traffic was busier than in S01 and S03 (Figure S1 and S4). Route density showed seasonal peaks, with higher values typically in summer months, likely due to increased commercial shipping. A major spike in spring 2022, where the 14-day moving average Chl-a exceeded 1 mg/m^3, was possibly linked to an episodic event such as dust deposition. Despite increased shipping, there was no clear long-term trend in Chl-a or TSM, suggesting limited direct impact from route density alone, or that impacts were episodic or masked by natural variability. For open sea areas, S05-S10, the typical seasonal pattern prevailed with median Chl-a concentration of approximately 0.2 mg/m^3 throughout winter and early spring and around 0.1 mg/m^3 during summer months Fig. 4).

.5. *Impact of shipping on Chl-a levels*

In addition to selected *open sea* and *coastal* areas, Chl-a and TSM levels were investigated along major maritime *routes* (R01-R15) across the study area. Monthly average Chl-a concentrations along the routes showed the expected pattern of Mediterranean in almost all routes where Chl-a concentrations were higher in winter and lower in summer (Fig. 4-bottom). Routes R08 and R02 are not in the Mediterranean, but from the Canakkale Strait through the Aegean Sea, and the reason for the slightly higher variability in Chl-a concentrations could be explained by the fact that these routes are impacted by the mucilage event in the Sea

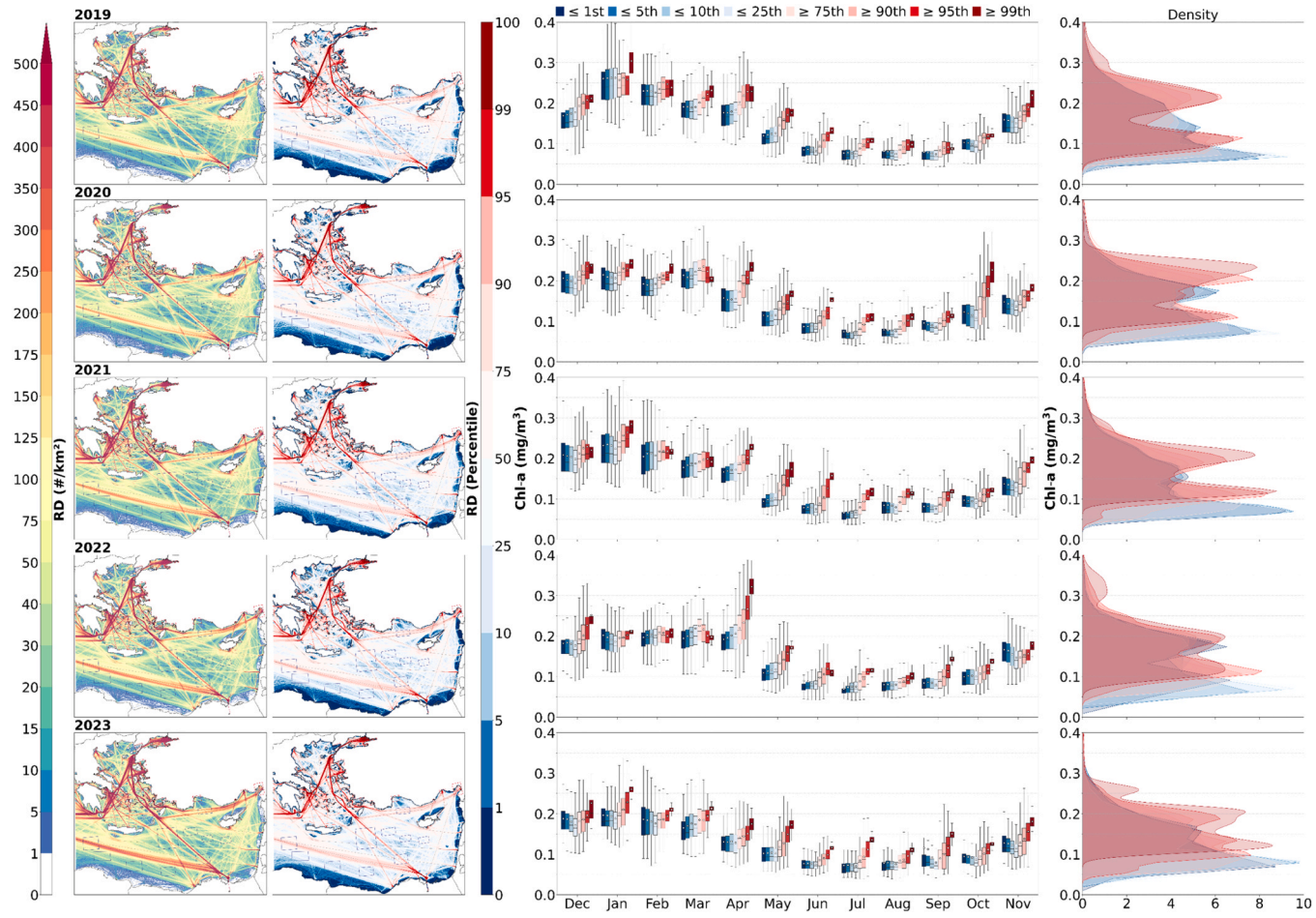

Fig. 5. Annual route density (RD) percentile distributions (left), monthly average Chl-a levels for percentile categories (open sea with >200 m bathymetry) (center) with their yearly Chl-a distributions (right).

of Marmara, as it can be observed in the Chl-a spike in Aug 2021, for both routes. The route densities increased slightly every year except for a drop in mid-2020, possibly linked to COVID-19 pandemic impacts on shipping (Fig. 5, Figure S4). As a general trend in all routes, route density showed a cyclic trend with decreases in winter and increases in summer which did not overlap with the Chl-a trends observed along the routes.

Overall, Chl-a concentrations along these routes followed expected seasonal trends with increases in winter and decreases in summer (Fig. 4, Figure S4). In 2021, some routes (R02, R07, R08) showed elevated Chl-a (Fig. 4), likely influenced by mucilage events and wildfires. A distinct spike appeared almost all routes in spring 2022, suggesting a potential widespread bloom event, possibly triggered by dust transport.

Route density of the Suez Canal-Canakkale Strait route (R04) passing from Mediterranean and Aegean Sea (Fig. 1) increased in mid to late 2023. Chl-a concentrations were moderate levels in most years (0.1–0.3 mg/m^3), typical of mesotrophic to oligotrophic waters in the Aegean-Eastern Mediterranean. The Aliaga-Canakkale Strait route (R08) showed higher Chl-a concentrations than other routes, likely due to its proximity to the shoreline and industrial activity. The Tasucu-Girne route (R06) also exhibited relatively high values, which could be influenced by nutrient inputs from the Goksu Delta and Tasucu Port (C12) where cargo ships carrying livestock dock. Similarly, the Izmir-Mediterranean route (R07) showed elevated Chl-a probably due to urban runoff and wastewater discharges from the Izmir metropolitan area (Fig. 4, Figure S4).

The Mediterranean-Suez Canal route (R01) exhibited lower monthly average Chl-a concentrations, around 0.1 mg/m^3, as it primarily passes through open sea areas. In contrast, route R04, which also traverses the Suez Canal but connects to or from the Canakkale Strait, showed higher Chl-a levels than R01, likely due to the influence of the Aegean Islands. The Mediterranean-Canakkale Strait route (R02) was the busiest route in the study area with the highest route density and displayed relatively higher Chl-a concentrations and its proximity to coastal and land-influenced regions might have affected these high levels (Figure S4).

The fact that the cyclic patterns of RD and Chl-a concentrations did not overlap implied no direct relation between the RD and Chl-a concentrations on the selected routes. Nevertheless, it is important to state several limitations of this approach. The first one is related with the fact that the satellite retrievals for the whole route may not be representing the same day, since it usually takes two-three days for GCOM to cover the whole study region. The second limitation is that the route zones selected with fixed width along the routes did not have uniformly high RD regions due to slightly changing of the individual ship routes. These limitations impact the average Chl-a concentrations which make it harder to observe the relationship. In addition, the type, size and age of the ships as well as the type of cargo may affect how much nutrient is discharged. For example, RD alone cannot distinguish between cargo ships carrying livestock and other types of cargo, although ships with more than 20,000 animals onboard are known to cause serious smell problems due to NH_3 emissions. The significant animal waste of these carriers could be responsible for N input from ship wastewater discharges, and also atmospheric N deposition from NH_3 emissions.

The route-based assessment of Chl-a did not indicate a significant relationship. Therefore, a more thorough investigation on the possible

nutrient sources in the open sea areas was needed. Since coastal areas are excluded for the areas S01-S10, the observed increase in Chl-a concentrations in these open sea areas necessitates that either natural sources via atmospheric deposition or ship wastewater discharges as possible nutrient sources in addition to the known impact of eddies (Siokou et al., 2025) favoring vertical exchange of water masses thus transporting nutrients. Therefore, two approaches were further used. Firstly, to assess the possible effect of shipping on Chl-a concentrations, a grid-based more precise spatial assessment was used, where Chl-a concentrations in the Mediterranean open sea areas for the 5-year period were joined with RD percentiles. The percentile ranges of ≤ 1, ≤ 5, ≤ 10 and ≤ 25, and ≥ 75, ≥ 90, ≥ 95 and ≥ 99 were selected to represent low and high shipping intensity regions, respectively. The mean and median Chl-a along with their distributions were investigated for each percentile category (Fig. 5 and Figure S6). *Mann-Whitney U-Test* was used to check the percentile RD and Chl-a relationship in order to determine significant differences in Chl-a levels among all individual percentile groups. When percentiles of ≤ 25, and ≥ 75 were compared, all datasets showed statistically significant differences indicating higher levels in ≥ 75 except Jan 2019. The probability density distributions also showed shifts in Chl-a levels for higher percentile ranges (Figure S6) suggesting that the underlying datasets were statistically different.

For all five years, between April and November, it was evident that the routes corresponding to high shipping intensity have significantly higher Chl-a concentration compared with those with low intensity (Fig. 5). The enhancements were especially noticeable in months with low Chl-a levels (May-Oct). The Chl-a levels increase with high correlation as the upper percentile categories increase (Figure S6). This difference was also observed in most other months with higher Chl-a concentrations except four months (Mar 2020, Feb 2021, Feb 2022 and Mar 2022) within all years.

The use of grid-base categorization instead of fixed width route zones proved to be successful, and the results indicated that in the open sea areas where the route density was high also had high Chl-a concentrations suggesting a strong link between shipping activity and increased phytoplankton biomass for the first time in the literature to our knowledge.

.6. *Episodic investigations on factors impacting Chl-a levels*

The investigation of different coastal and open sea areas for five years demonstrated the spatio-temporal variations and extreme event impacts on daily and monthly average Chl-a concentrations. Some of these events were associated with land-based sources, and extreme mucilage event. However, the remaining high Chl-a levels away from the coast, requires further attention. In this context, a second approach was designed to determine the possible sources of nutrients in the open sea leading to high Chl-a concentrations. Three specific episodes focusing on one anthropogenic (livestock carriers) and two natural sources (wildfires and dust transport) were determined (Table 2), and investigated spatially and temporally in detail.

In order to determine whether the mean Chl-a levels over the periods differ significantly before and after the selected events for each subregion *a paired t-test* was conducted, as applied in previous Chl-a studies (Kotta and Kitsiou, 2019b). According to results, differences between all subregions and periods were statistically significant at the 95 % confidence level ($p < 0.05$), except S08 between wildfire episode and its post period. Then, corresponding effect sizes were computed as Cohen's d to assess the strength of these differences. The results of the statistical analysis (Table S1) and the probability distributions of Chl-a distributions of pre, post and episodes for all subregions (Figure S9) showed significant differences.

The strong positive correlation of RD with Chl-a levels in the open seas of the Eastern Mediterranean (Figure S6), especially in the months with limited nutrient availability indicated the impact of wastewater from ships. Livestock carriers, in particular, along with their high capacity exceeding 20,000 animals can be a significant nutrient source in the open sea. The arrival and departure of the livestock carriers along with their cargo capacities to the ports of Mersin and Tasucu were investigated for the most recent year 2023 with daily Chl-a concentrations of S01, because these carriers follow the route R15. The spatial distribution of the Chl-a in the selected episode indicated higher levels around S01 reaching up to 300 % increases compared to both pre- and post- intervals (Fig. 6). These areas with significant increases coincide with the routes of livestock carriers.

In remote ocean ecosystems, aerosol deposition represents an essential source of nutrients for primary production, especially from significant natural sources of wildfires and dust storms (Hamilton et al., 2025). As an example, 2019–2020 Australian wildfires caused widespread phytoplankton blooms in the Southern Ocean downwind of Australia (Tang et al., 2021; Wang et al., 2022). 2021 wildfire season was the second worst on record for EU since 2000, with particularly large wildfires in Türkiye in July-Aug 2021 (San-Miguel-Ayanz et al., 2021). Previous studies indicated wildfire plumes from Türkiye transported to the Mediterranean open sea regions with high levels of pollutants such as NO_2 and NH_3 (Eke et al., 2024; Saracoglu et al., 2025). The second episode was focused on these wildfires, and indicated up to 500 % increases compared to both pre- and post- intervals in the regions where the smoke plume was transported (Fig. 7). The high increases compared to pre- in the northern Aegean Sea close to Greece could also be explained by the intense wildfires in Greece. This enhancement was not observed in the post- averages, because the wildfires continued in Greece after the selected time interval.

In the western subregions (S02, S04, S05, S06, and S10), the impact of wildfires was more pronounced (Fig. 9 and Table S1) due to northeasterly winds that transported the plume toward the southwest (Eke et al., 2024). Among these, S02 experienced the strongest response, where the average Chl-a concentration increased from 0.07 mg/m^3 before the wildfires to 0.15 mg/m^3 during the event. Similarly, in S04, average Chl-a concentrations rose from 0.06 to 0.11 mg/m^3.

The highest monthly levels were observed in March 2022 with a hotspot in the south east of Crete, significantly higher than other years (Fig. 2). Investigation of daily MODIS real-time images, aerosol index (AI) and aerosol optical depth (AOD) products revealed significant dust transport over the Mediterranean around the same time (Figure S8). Thus, the third episode was focused on this dust event. The highest magnitude and widely spread increases were observed in this episode, especially in the southern regions of Crete (Fig. 8). The daily Chl-a concentrations were observed highest in S02 and S10. The comparison of the pre- episodic and post- average Chl-a levels were performed for selected open sea areas (S01–10) and the Eastern Mediterranean open sea region. The highest enhancements were observed during the dust event (E03) with consistent increases in all selected regions (Fig. 9).

All study subregions (S01-S10) were influenced by dust transport, leading to significant Chl-a enhancements. The most affected area was S04, where average Chl-a concentrations increased sharply from 0.19 mg/m^3 before the dust storm to 0.61 mg/m^3 during the event. In larger scale, the Eastern Mediterranean exhibited an increase in average Chl-a concentrations from 0.24 mg/m^3 to 0.40 mg/m^3. A comparison of the post-dust storm and storm periods revealed that the enhancements were strongest during the event itself. Even in the least affected region, S03, Chl-a concentrations increased from 0.16 to 0.24 mg/m^3 during the dust episode.

The average Chl-a during the dust event ranged between 1.09 and 3.19 times of the pre-average Chl-a concentrations with 1.68 times for the whole Eastern Mediterranean region. The ratios were even higher when compared with post-averages reaching 2.09 for the whole Eastern Mediterranean. Our findings were similar to previous studies finding enhancements in Chl-a concentrations due to dust storms from the Gobi Desert (692 % increase) in the Northwest Pacific (Li and Wang, 2024), and dust deposition from the Sahara and Syria (11–36 % increase) in the Black Sea (Varenik and Kalinskaya, 2021). The impact of wildfire can

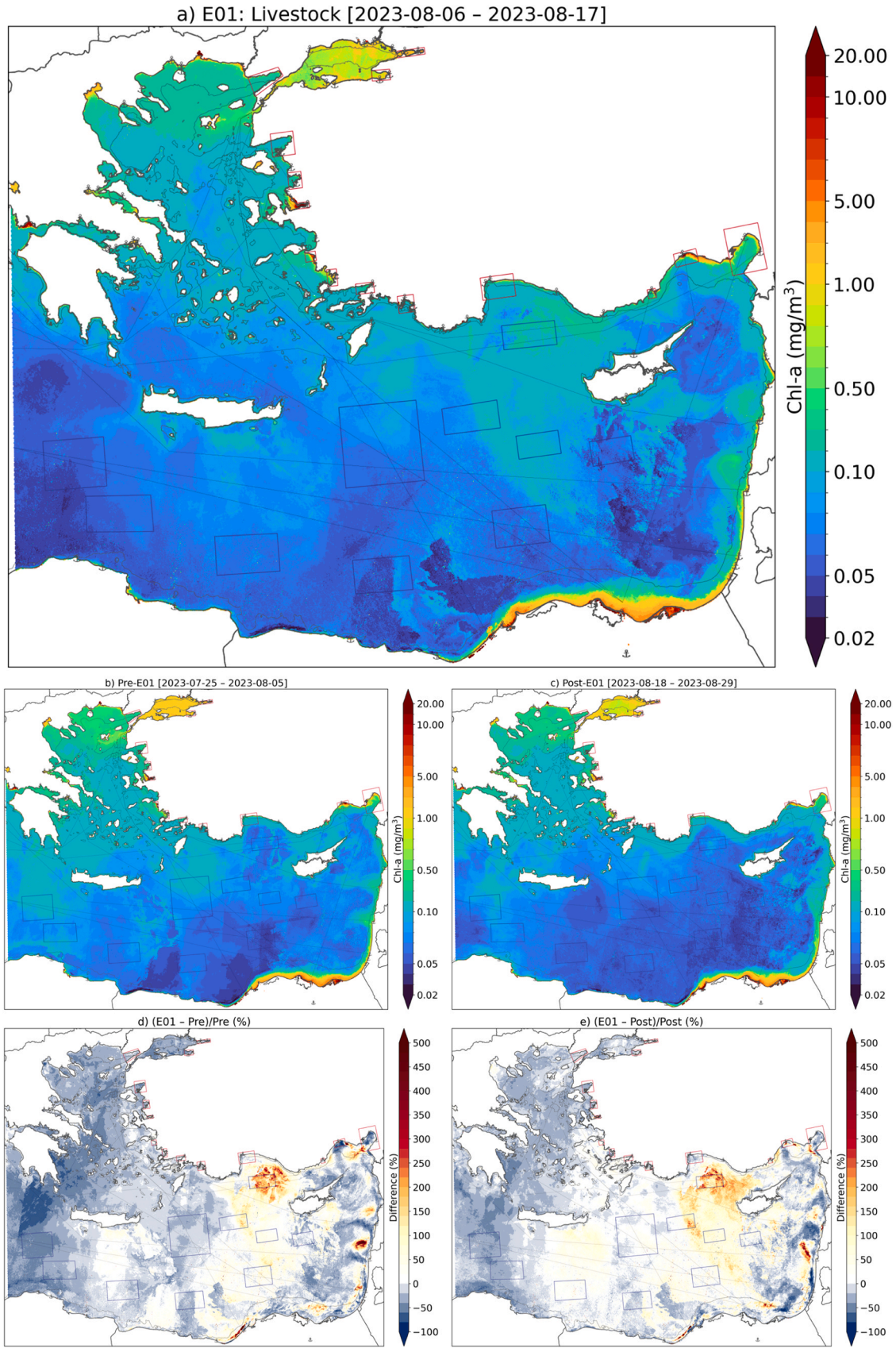

Fig. 6. Average Chl-a levels for E01: Livestock shipping (a) pre- (b), and post- (c) time intervals and the changes in between (d, e).

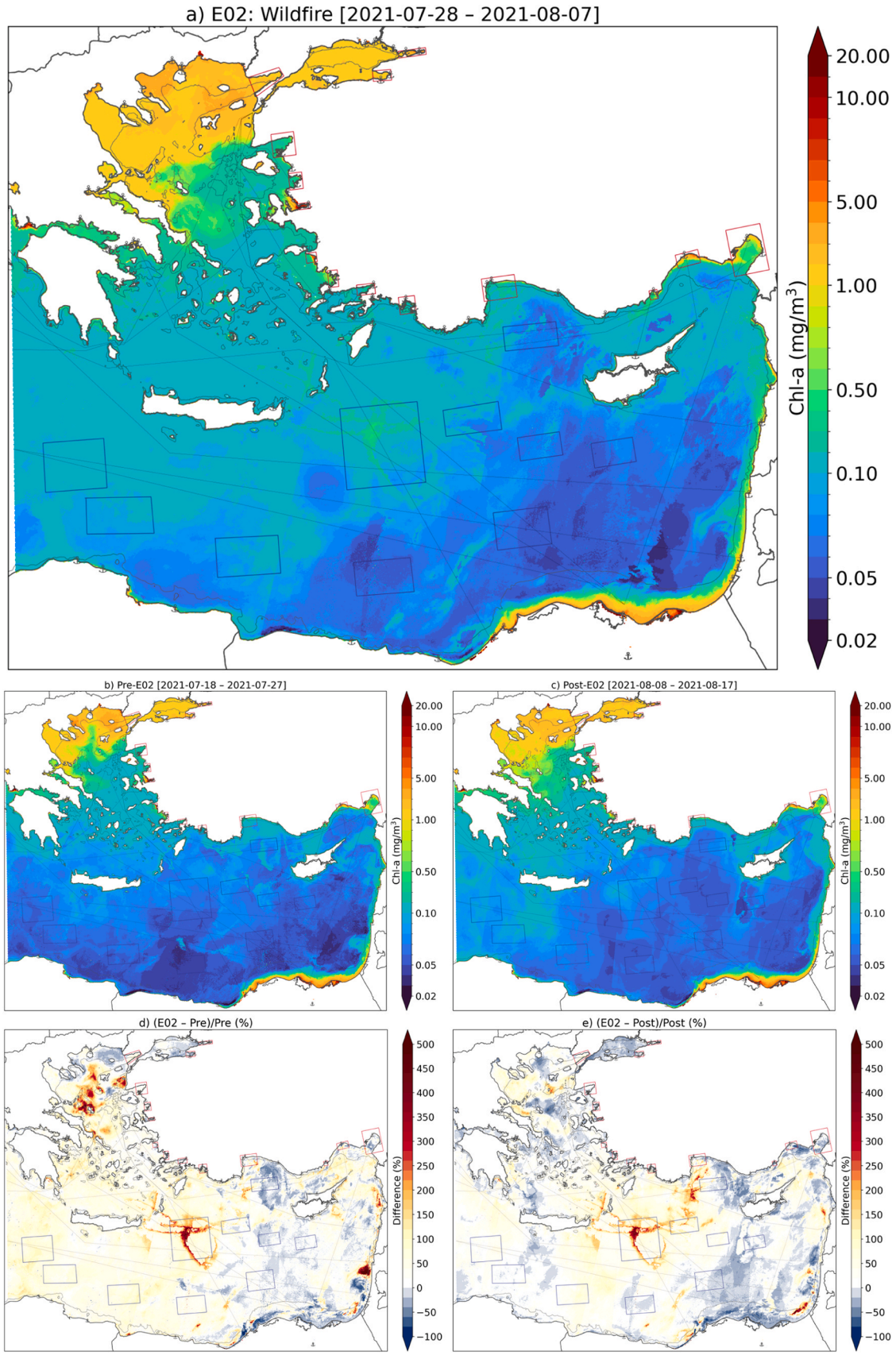

Fig. 7. Average Chl-a levels for E02: Wildfire (a), pre- (b), and post- (c) time intervals and the changes in between (d, e).

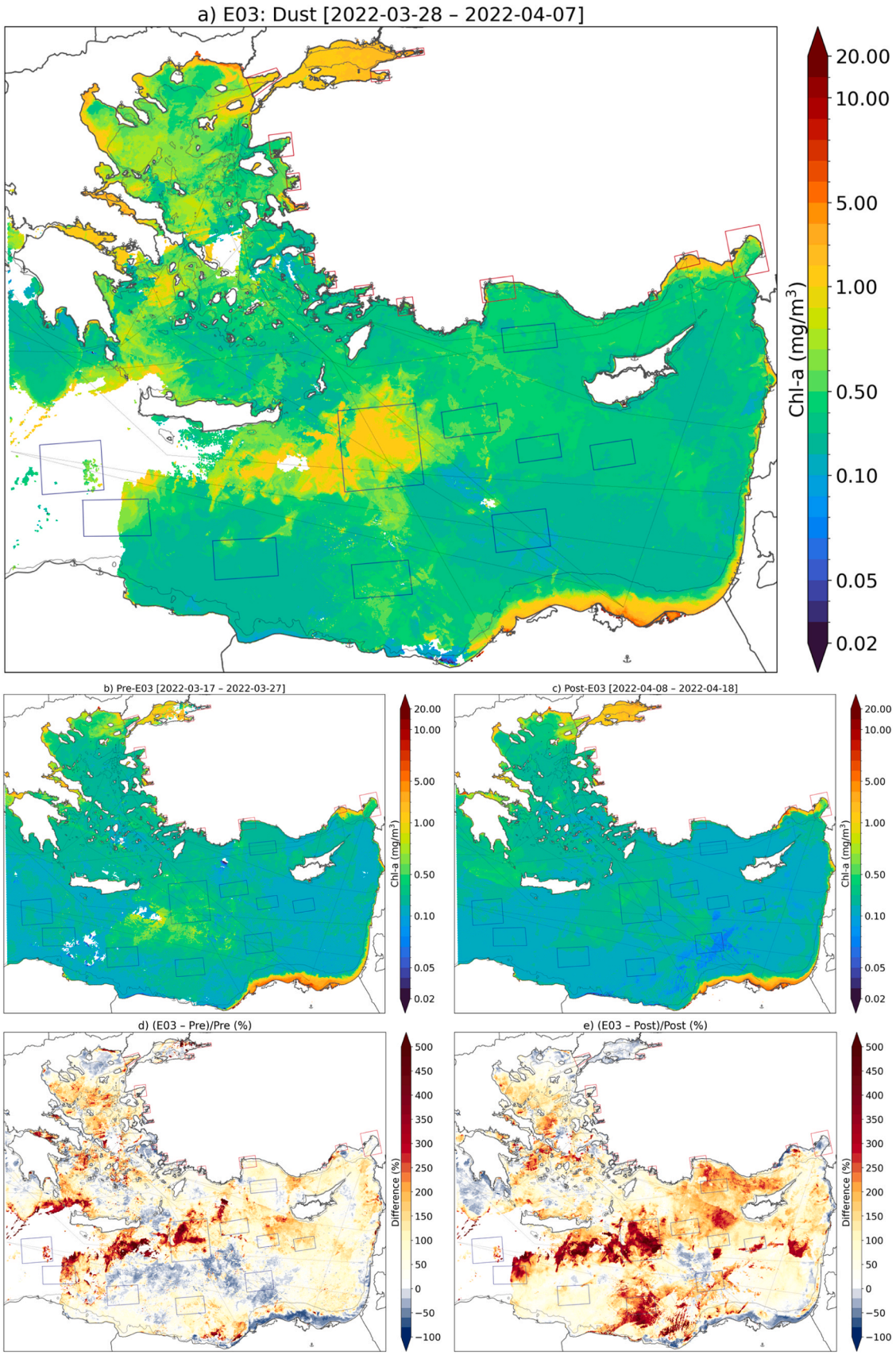

Fig. 8. Average Chl-a levels for E03: Dust (a) pre- (b), and post- (c) time intervals and the changes in between (d, e).

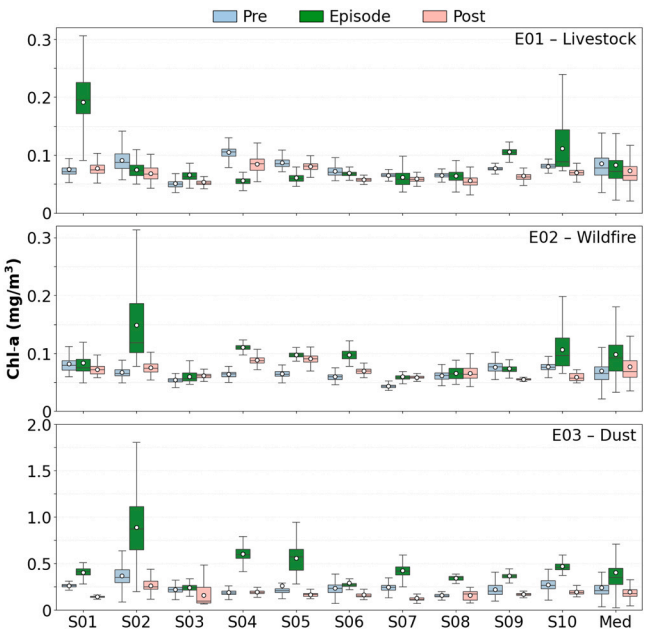

Fig. 9. Average Chl-a levels of the selected open sea areas and the Eastern Mediterranean for the selected episodes: livestock shipping, wildfire, and dust.

also be observed in the overall averages with 1.42–1.28 times of pre- and post- respectively. The highest impacted regions showed up to approximately two times increase (S02). The impact of livestock episode was regional with very large enhancements in S01 and S10, reaching 2.5 times compared to both pre- and post- averages in S01 (Fig. 9).

4. Conclusions

Eutrophication used to be a freshwater problem but with increasing population leading to higher pollution ending in marine waters, increase in Chl-a levels in the seas and possible catastrophic events in the coastal areas are being observed. The climate change is expected to worsen these outcomes. In-situ measurements of Chl-a are not only laborious and costly limiting the number of measurements and resulting in less-than-proper monitoring studies, but are also not always available to general public. In our study, through satellite retrievals of Chl-a, the nutrient status of the Sea of Marmara, the Aegean Sea and the Eastern Mediterranean was investigated, showing more polluted coastal areas and the temporal trends of Chl-a. These results underline the importance of terrestrial sources and similar approaches could be used to check the effect of policies to decrease pollution such as installing and properly operating wastewater treatment plants, particularly for hotspots such as Izmir and Izmit for coastal areas. The thorough investigation of temporal and spatial changes of Chl-a levels in open seas around Türkiye also acts as a base to compare future negative or positive effects of climate change or better environmental and maritime policies.

The correlation of high percentiles of route densities, indicating an association of high shipping intensities with Chl-a concentrations in the open sea is an important finding and can further be improved with inclusion of more detailed info on ships. Similarly, the addition of hydrologic information and sea surface temperatures may provide a way to anticipate the effect of nutrient discharges and emissions originating from ships. In addition, the temporal and spatial Chl-a data could be used as a proxy parameter for other types of pollution such as micro-pollutants and microplastics, and provide an essential tool in designing monitoring studies on those pollutants as well.

The impact of dust storms was with the highest magnitude and most widespread Chl-a enhancements, whereas wildfire and livestock episodes showed relatively lower and regional enhancements. Nevertheless, all of the episodes showed consistently higher levels compared to pre- and post- time intervals. The comparisons were specific to the selected episodes, and are not to be taken as a general comparison of these two phenomena (wildfire and dust storm). Because the seasons were different in wildfire and dust episodes, several other factors such as mixed layer depth and surface nutrients concentration vary and can contribute to Chl-a enhancements. The inevitable natural events of wildfires and dust storms are expected to increase in the future with the impacts of climate change in the Mediterranean, indicating more effort is needed to quantify and reduce the possible anthropogenic impacts such as shipping.

Funding

This study was partially supported by Istanbul Technical University Scientific Research Projects Coordination Unit (ITU BAP) under the grant number MDK-2023-45113 (Graduate Thesis Project).

CRediT authorship contribution statement

Burcak Kaynak: Writing – review & editing, Writing – original draft, Supervision, Resources, Methodology, Investigation, Conceptualization. **Muhittin Gunes Onay:** Writing – original draft, Methodology, Investigation, Formal analysis, Conceptualization. **Serra Saracoglu:** Writing – review & editing, Visualization, Investigation, Formal analysis. **Elif Pehlivanoglu:** Writing – review & editing, Writing – original draft, Investigation, Conceptualization.

Declaration of Competing Interest

The authors declare that they have no known competing financial interests or personal relationships that could have appeared to influence the work reported in this paper.

Acknowledgments

We thank Japan Aerospace Exploration Agency (JAXA), and European Marine Observation and Data Network (EMODnet) for providing data as open source. This study was partially supported by Istanbul Technical University Scientific Research Projects Coordination Unit (ITU BAP) under the grant number MDK-2023–45113 (Graduate Thesis Project).

Appendix A. Supporting information

Supplementary data associated with this article can be found in the online version at doi:10.1016/j.rsma.2026.104858.

Data availability

Data will be made available on request.

References

Action Plan, 2020. Mugla Marine Waste Action Plan. Republic of Türkiye Ministry of Environment, Urbanization and Climate Change, Mugla Provincial Directorate of Environment. ⟨https://webdosya.csb.gov.tr/db/mugla/menu/mugla-ili-deniz-copleri-il-eylem-plani_20200117025608.pdf⟩. Accessed June 16 2025.

Amitai, Y., Lehahn, Y., Lazar, A., Heifetz, E., 2010. Surface circulation of the eastern Mediterranean Levantine basin: Insights from analyzing 14 years of satellite altimetry data. J. Geophys. Res. Oceans 115 (10). https://doi.org/10.1029/2010JC006147.

Androulidakis, Y.S., Krestenitis, Y.N., Psarra, S., 2017. Coastal upwelling over the North Aegean sea: observations and simulations. Cont. Shelf Res. 149, 32–51. https://doi.org/10.1016/J.CSR.2016.12.002.

Aulinger, A., Matthias, V., Zeretzke, M., Bieser, J., Quante, M., Backes, A., 2016. The impact of shipping emissions on air pollution in the greater North Sea region - Part 1: current emissions and concentrations. Atmos. Chem. Phys. 16 (2), 739–758. https://doi.org/10.5194/acp-16-739-2016.

Balkıs Özdelice, N., Durmuş, T., Balcı, M., 2023. The role of phytoplankton in the formation of mucilage observed in the sea of Marmara from past to present. Mucilage Problem in the Sea of Marmara. Istanbul University Press, pp. 143–164. https://doi.org/10.26650/b/ls32.2023.003.06.

Bardakçı Şener, B., Tıraşın, E.M., 2024. A preliminary study into the influence of filtration on phytoplankton dynamics in an oligotrophic marine fish farm environment. Ege J. Fish. Aquat. Sci. 41 (1), 16–25. https://doi.org/10.12714/egejfas.41.1.03.

Bigio, L., Mayol-Bracero, O.L., Santos, G., Fishman, A., Angert, A., 2020. Are the phosphate oxygen isotopes of Saharan dust a robust tracer of atmospheric P source? Atmos. Environ. 235, 117561. https://doi.org/10.1016/J.ATMOSENV.2020.117561.

Bilgin Güney, C., Kinaci, O.K., 2024. Ecological effects and mitigation strategies for underwater noise from shipping activities. Ships Offshore Struct. 1–13. https://doi.org/10.1080/17445302.2024.2443083.

Bossard, C., Bonnemains, J., 2024. 64 EU-approved livestock carriers. Robin des Bois & Animal Welfare Foundation e.V. ⟨https://www.animal-welfare-foundation.org/files/downloads/Report_64-livestock_AWF_RobindesBois_FINAL_March24-BD.pdf⟩. Accessed June 16 2025..

Browning, T.J., Moore, C.M., 2023. Global analysis of ocean phytoplankton nutrient limitation reveals high prevalence of co-limitation. Nat. Commun. 14 (1). https://doi.org/10.1038/s41467-023-40774-0.

Charette, T., Prepas, E.E., 2003. Wildfire impacts on phytoplankton communities of three small lakes on the Boreal Plain, Alberta, Canada: a paleolimnological study. Can. J. Fish. Aquat. Sci. 60 (5), 584–593. https://doi.org/10.1139/f03-049.

Chen, D., Fu, X., Guo, X., Lang, J., Zhou, Y., Li, Y., Liu, B., Wang, W., 2020. The impact of ship emissions on nitrogen and sulfur deposition in China. Sci. Total Environ. 708, 134636. https://doi.org/10.1016/j.scitotenv.2019.134636.

Chen, J., Wang, K., Li, X., Zhao, X., Cheng, X., Liu, Z., Zhang, J., Zhang, S., 2024. Remote sensing inversion of water quality parameters (TSM, Chl-a, and CDOM) in subtidal seaweed beds and surrounding waters. Ecol. Indic. 167, 112716. https://doi.org/10.1016/J.ECOLIND.2024.112716.

Chen, Q., Wu, W., Guo, Y., Li, J., Wei, F., 2022. Environmental impact, treatment technology and monitoring system of ship domestic sewage: a review. Sci. Total Environ. 811, 151410. https://doi.org/10.1016/J.SCITOTENV.2021.151410.

Demir, B., 2022. Investigation of Opportunity to Use Sentinel-3 OLCI Data in the Determination of Chlorophyll-a Concentration at Regional Scale. Istanbul Technical University, Master Thesis.

Eke, M., Cingiroglu, F., Kaynak, B., 2024. Investigation of 2021 wildfire impacts on air quality in southwestern Turkey. Atmos. Environ. 325, 120445. https://doi.org/10.1016/J.ATMOSENV.2024.120445.

El Hourany, R., Fadel, A., Gemayel, E., Abboud-Abi Saab, M., Faour, G., 2017. Spatio-temporal variability of the phytoplankton biomass in the Levantine basin between 2002 and 2015 using MODIS products. Oceanologia 59 (2), 153–165. https://doi.org/10.1016/J.OCEANO.2016.12.002.

EMODnet. 2025a. EMODnet Digital Bathymetry (DTM 2024). EMODnet Bathymetry Consortium ⟨https://doi.org/10.12770/cf51df64-56f9-4a99-b1aa-36b8d7b743a1⟩. Accessed February 3 2025.

EMODnet. 2025b. *EMODnet human activities, EMSA route density map.* ⟨https://emodnet.ec.europa.eu/geonetwork/srv/eng/catalog.search#/metadata/74eef9c6-13fe-4630-b935-f26871c8b661⟩. Accessed February 3 2025.

Freilich, M.A., Flierl, G., Mahadevan, A., 2022. Diversity of growth rates maximizes phytoplankton productivity in an Eddying ocean. Geophys. Res. Lett. 49 (3). https://doi.org/10.1029/2021GL096180.

Gaballa Altohame Jalgaif, G., Ali Mahgoub Idris, S., Ali Maarouf, R., Moursy Attia, A., Mahmoud El-Naggar, M., 2019. Effect of heavy metals and nutrients levels of ballast waters in commercial ships on chemical quality status of seawater of the Tobruk-Libya Gulf. Am. J. Environ. Resour. Econ. 4 (4), 121. https://doi.org/10.11648/j.ajere.20190404.11.

Giannaros, T.M., Papavasileiou, G., Lagouvardos, K., Kotroni, V., Dafis, S., Karagiannidis, A., Dragozi, E., 2022. Meteorological analysis of the 2021 extreme wildfires in greece: lessons learned and implications for early warning of the potential for pyroconvection. Atmosphere 13 (3). https://doi.org/10.3390/atmos13030475.

Gössling, S., Meyer-Habighorst, C., Humpe, A., 2021. A global review of marine air pollution policies, their scope and effectiveness. Ocean Coast. Manag. 212, 105824. https://doi.org/10.1016/J.OCECOAMAN.2021.105824.

G-PORTAL. 2025a. Global Portal System. ⟨https://gportal.jaxa.jp/gpr/?lang=en⟩. Accessed April 14 2025.

G-PORTAL. 2025b. Earth Observation Data Conversion Tool. ⟨https://gportal.jaxa.jp/gpr/information/tool?lang=en#GCOM-C⟩. Accessed April 14 2025.

Gucel, M.U., Sakalli, A., 2024. Analyzing the Mediterranean sea's dynamic current system and modeling of renewable current energy potential. J. Mar. Sci. Eng. 12 (4). https://doi.org/10.3390/jmse12040671.

Hamilton, D.S., Perron, M.M.G., Bond, T.C., Bowie, A.R., Buchholz, R.R., Guieu, C., Ito, A., Maenhaut, W., Myriokefalitakis, S., Olgun, N., Rathod, S.D., Schepanski, K., Tagliabue, A., Wagner, R., Mahowald, N.M., 2025. Earth, Wind, fire, and pollution: aerosol nutrient sources and impacts on ocean biogeochemistry. 58, 4. https://doi.org/10.1146/annurev-marine-031921.

He, X., Bai, Y., Pan, D., Huang, N., Dong, X., Chen, J., Chen, C.T.A., Cui, Q., 2013. Using geostationary satellite ocean color data to map the diurnal dynamics of suspended particulate matter in coastal waters. Remote Sens. Environ. 133, 225–239. https://doi.org/10.1016/J.RSE.2013.01.023.

Hu, C., Lee, Z., Franz, B., 2012. Chlorophyll a algorithms for oligotrophic oceans: a novel approach based on three-band reflectance difference. J. Geophys. Res. Oceans 117 (C1). https://doi.org/10.1029/2011JC007395.

Jäger, C.G., Diehl, S., Schmidt, G.M., 2008. Influence of water-column depth and mixing on phytoplankton biomass, community composition, and nutrients. Limnol. Oceanogr. 53 (6), 2361–2373. https://doi.org/10.4319/lo.2008.53.6.2361.

JAXA. (2022). SGLI L2 Ocean Products (Version 3.0) Validation Results. ⟨https://suzaku.eorc.jaxa.jp/GCOM_C/data/validation.html⟩. Accessed April 14 2025.

Kala, C.P., 2023. Environmental and socioeconomic impacts of forest fires: a call for multilateral cooperation and management interventions. Nat. Hazards Res. 3 (2), 286–294. https://doi.org/10.1016/J.NHRES.2023.04.003.

Kim, S., Lee, D., Kim, M., Jang, H.K., Park, S., Kim, Y., Kim, J., Park, J.W., Joo, H., Lee, S. H., 2024. Seasonal patterns and bloom dynamics of phytoplankton based on satellite-derived chlorophyll-a in the Eastern Yellow Sea. Mar. Environ. Res. 199. https://doi.org/10.1016/j.marenvres.2024.106605.

Kotta, D., Kitsiou, D., 2019a. Chlorophyll in the Eastern Mediterranean sea: correlations with environmental factors and trends. Environ. MDPI 6 (8). https://doi.org/10.3390/environments6080098.

Kotta, D., Kitsiou, D., 2019b. Exploring possible influence of dust episodes on surface marine chlorophyll concentrations. J. Mar. Sci. Eng. 7 (2), 50. https://doi.org/10.3390/jmse7020050.

Kournopoulou, A., Kikaki, K., Varkitzi, I., Psarra, S., Assimakopoulou, G., Karantzalos, K., Raitsos, D.E., 2024. Atlas of phytoplankton phenology indices in selected Eastern Mediterranean marine ecosystems. Sci. Rep. 14 (1). https://doi.org/10.1038/s41598-024-60792-2.

Kramer, S.J., Bisson, K.M., Fischer, A.D., 2020. Observations of phytoplankton community composition in the Santa Barbara channel during the thomas fire. J. Geophys. Res. Oceans 125 (12). https://doi.org/10.1029/2020JC016851.

Lappalainen, S.-T., Tapaninen, U., Kotta, J., 2024. Nitrogen and phosphorus discharges from cargo ships' black and grey waters—a case study of a Baltic Sea Port. Oceans 5 (3), 560–570. https://doi.org/10.3390/oceans5030032.

Li, Y., Wang, W., 2024. Long-range transport of a dust event and impact on marine chlorophyll-a concentration in April 2023. Remote Sens. 16 (11), 1883. https://doi.org/10.3390/rs16111883.

Liu, D., Zhou, C., Keesing, J.K., Serrano, O., Werner, A., Fang, Y., Chen, Y., Masque, P., Kinloch, J., Sadekov, A., Du, Y., 2022. Wildfires enhance phytoplankton production in tropical oceans. Nat. Commun. 13 (1). https://doi.org/10.1038/s41467-022-29013-0.

Luang-on, J., Siswanto, E., Ogata, K., Toratani, M., Buranapratheprat, A., Leenawarat, D., Ishizaka, J., 2024. Enhancing the reliability of GCOM-C/SGLI data for red tide detection in the upper Gulf of Thailand. Remote Sens. Lett. 15 (10), 1096–1106. https://doi.org/10.1080/2150704X.2024.2406032.

Mamoutos, I., Zervakis, V., Tragou, E., Karydis, M., Frangoulis, C., Kolovoyiannis, V., Georgopoulos, D., Psarra, S., 2017. The role of wind-forced coastal upwelling on the thermohaline functioning of the North Aegean Sea. Cont. Shelf Res. 149, 52–68. https://doi.org/10.1016/J.CSR.2017.05.009.

Martin, D., Tomida, M., Meacham, B., 2016. Environmental impact of fire. Fire Sci. Rev. 5 (1), 5. https://doi.org/10.1186/s40038-016-0014-1.

Maslukah, L., Ismunarti, D.H., Widada, S., Sandi, N.F., Prayitno, H.B., 2022. The interaction of chlorophyll-a and total suspended matter along the Western Semarang Bay, Indonesia, based on measurement and retrieval of sentinel 3. J. Ecol. Eng. 23 (10), 191–201. https://doi.org/10.12911/22998993/152428.

Meng, Q., Yan, C., Li, R., Zhang, T., Zheng, M., Liu, Y., Zhang, M., Wang, G., Du, Y., Shang, C., Fu, P., 2023. Variations of PM2.5-bound elements and their associated effects during long-distance transport of dust storms: insights from multi-sites observations. Sci. Total Environ. 889, 164062. https://doi.org/10.1016/J.SCITOTENV.2023.164062.

MoEUCC. 2022a. Marine quality bulletin for Aegean Sea. ⟨https://webdosya.csb.gov.tr/db/ced/icerikler/den-z-kal-tes–bulten–2022_ege_den-z–20230720163802.pdf⟩. Accessed September 3 2025.

MoEUCC. 2022b. Marine quality bulletin for Mediterranean. ⟨https://webdosya.csb.gov.tr/db/ced/icerikler/den-z-kal-tes–bulten–2022_akden-z-20230720163831.pdf⟩. Accessed September 3 2025.

MoEUCC. 2022c. Marine quality bulletin for Sea of Marmara. ⟨https://webdosya.csb.gov.tr/db/ced/icerikler/den-z-kal-tes–bulten–2022_marmara_den-z–20230720163728.pdf⟩. Accessed September 3 2025.

Nguyen, H.D., Leys, J., Riley, M., White, S., Azzi, M., Trieu, T., Salter, D., Ji, F., Nguyen, H., Chang, L.T.C., Monk, K., Firth, J., Fuchs, D., Barthelemy, X., 2024. Effects of dust storm and wildfire events on phytoplankton growth and carbon sequestration in the Tasman Sea, Southeast Australia. Atmosphere 15 (3). https://doi.org/10.3390/atmos15030337.

Nishioka, J., Hirawake, T., Nomura, D., Yamashita, Y., Ono, K., Murayama, A., Shcherbinin, A., Volkov, Y.N., Mitsudera, H., Ebuchi, N., Wakatsuchi, M., Yasuda, I., 2021. Iron and nutrient dynamics along the East Kamchatka Current, western Bering Sea Basin and Gulf of Anadyr. Prog. Oceanogr. 198, 102662. https://doi.org/10.1016/J.POCEAN.2021.102662.

O'Reilly, J., Maritorena, S., Mitchell, B.G., Siegel, D.A., Carder, K.L., Garver, S.A., Kahru, M., McClain, C.R., 2000. Ocean color chlorophyll a algorithms for SeaWiFS, OC2, and OC4: Version 4. SeaWiFS Postlaunch Calibration and Validation Analyses, 11, pp. 9–23.

Oms, L., Messié, M., Poggiale, J.C., Grégori, G., Doglioli, A., 2024. Fine-scale phytoplankton community transitions in the oligotrophic ocean: a Mediterranean Sea case study. J. Mar. Syst. 246, 104021. https://doi.org/10.1016/J.JMARSYS.2024.104021.

Poulain, P.M., Menna, M., Mauri, E., 2012. Surface geostrophic circulation of the mediterranean sea derived from drifter and satellite altimeter data. J. Phys. Oceanogr. 42 (6), 973–990. https://doi.org/10.1175/JPO-D-11-0159.1.

Princewill, O.I., Odoemelam, V.U., Omede, A.A., Emenalom, O.O., 2012. Livestock waste and its impact on the environment. Artic. Sci. J. Rev. 1 (1), 17–32.

Pseftogkas, A., Koukouli, M.E., Skoulidou, I., Balis, D., Meleti, C., Stavrakou, T., Falco, L., van Geffen, J., Eskes, H., Segers, A., Manders, A., 2021. A new separation methodology for the maritime sector emissions over the Mediterranean and Black Sea regions. Atmosphere 12 (11). https://doi.org/10.3390/atmos12111478.

Raudsepp, U., Maljutenko, I., Kõuts, M., Granhag, L., Wilewska-Bien, M., Hassellöv, I.M., Eriksson, K.M., Johansson, L., Jalkanen, J.P., Karl, M., Matthias, V., Moldanova, J., 2019. Shipborne nutrient dynamics and impact on the eutrophication in the Baltic Sea. Sci. Total Environ. 671, 189–207. https://doi.org/10.1016/j.scitotenv.2019.03.264.

Raut, J.C., Law, K.S., Onishi, T., Daskalakis, N., Marelle, L., 2022. Impact of shipping emissions on air pollution and pollutant deposition over the Barents Sea. Environ. Pollut. 298. https://doi.org/10.1016/j.envpol.2022.118832.

Salem, S.I., Toratani, M., Higa, H., Son, S., Siswanto, E., Ishizaka, J., 2025. Long-Term Evaluation of GCOM-C/SGLI Reflectance and Water Quality Products: Variability Among JAXA G-Portal and JASMES. Remote Sens. 17 (2), 221. https://doi.org/10.3390/rs17020221.

Salgado-Hernanz, P.M., Racault, M.F., Font-Muñoz, J.S., Basterretxea, G., 2019. Trends in phytoplankton phenology in the Mediterranean Sea based on ocean-colour remote sensing. Remote Sens. Environ. 221, 50–64. https://doi.org/10.1016/j.rse.2018.10.036.

San-Miguel-Ayanz, J., Durrant, T., Boca, R., Maianti, P., Liberta`, G., Artes Vivancos, T., Jacome Felix Oom, D., Branco, A., De Rigo, D., Ferrari, D., Pfeiffer, H., Grecchi, R. and Nuijten, D.., Advance report on wildfires in Europe, Middle East and North Africa 2021, EUR 31028 EN, Publications Office of the European Union, Luxembourg, 2022, ISBN 978-92-76-49633-5, doi:10.2760/039729,JRC128678.

Saracoglu, S., Alban, A.M., Tokgoz, S., Kaynak, B., 2025. Investigation of the intense wildfire events and NH3 levels over the Eastern Mediterranean. EGU General Assembly 2025, Vienna, Austria, 27 Apr–2 May 2025, EGU25-17646, https://doi.org/10.5194/egusphere-egu25-17646.

Shu, Y., Wang, X., Huang, Z., Song, L., Fei, Z., Gan, L., Xu, Y., Yin, J., 2022. Estimating spatiotemporal distribution of wastewater generated by ships in coastal areas. Ocean Coast. Manag. 222, 106133. https://doi.org/10.1016/J.OCECOAMAN.2022.106133.

Siokou, I., Simantiris, N., Christou, E.D., Theocharis, A., 2025. Episodic deep vertical mixing in the Rhodes gyre (Mediterranean Sea) triggers an exceptional mesozooplankton outburst. Prog. Oceanogr. 235. https://doi.org/10.1016/j.pocean.2025.103496.

Son, S., Campbell, J., Dowell, M., Yoo, S., Noh, J.-H., 2005. Primary production in the Yellow Sea determined by ocean color remote sensing. Mar. Ecol. Prog. Ser. 303, 91–103. https://doi.org/10.3354/meps303091.

Suez Canal Authority. (2023). Suez Canal traffic statistics: Annual report 2023. Planning & Research Department, Information Center. ⟨https://www.suezcanal.gov.eg⟩. Accessed June 6 2025.

Sun, Y., Wang, D., Li, L., Ning, R., Yu, S., Gao, N., 2024. Application of remote sensing technology in water quality monitoring: From traditional approaches to artificial intelligence. Water Res. 267, 122546. https://doi.org/10.1016/J.WATRES.2024.122546.

Tang, W., Llort, J., Weis, J., Perron, M.M.G., Basart, S., Li, Z., Sathyendranath, S., Jackson, T., Sanz Rodriguez, E., Proemse, B.C., Bowie, A.R., Schallenberg, C., Strutton, P.G., Matear, R., Cassar, N., 2021. Widespread phytoplankton blooms triggered by 2019–2020 Australian wildfires. Nature 597 (7876), 370–375. https://doi.org/10.1038/s41586-021-03805-8.

Toratani, M. 2021. SGLI algorithm theoretical basis document: total suspended matter concentration. ⟨https://suzaku.eorc.jaxa.jp/GCOM_C/data/ATBD/ver2/V2ATBD_O3AB_TSM_Toratani_jp_r1.pdf⟩. Accessed April 14 2025.

Tükenmez, E., Altıok, H., 2022. Upwelling index calculations in the Aegean sea. Turk. J. Fish. Aquat. Sci. 22 (12). https://doi.org/10.4194/TRJFAS21621.

Tuzcu Kokal, A., Olgun, N., Musaoğlu, N., 2022. Detection of mucilage phenomenon in the Sea of Marmara by using multi-scale satellite data. Environ. Monit. Assess. 194 (8), 585. https://doi.org/10.1007/s10661-022-10267-6.

Van Leeuwen, S.M., Beecham, J.A., Garc\'\ia-Garc\'\ia, L.M., Thorpe, R., 2022. The Mediterranean Rhodes Gyre: modelled impacts of climate change, acidification and fishing. Mar. Ecol. Prog. Ser. 690, 31–50. https://doi.org/10.3354/meps14016.

Varenik, A.V., Kalinskaya, D.V., 2021. The effect of dust transport on the concentration of chlorophyll-a in the surface layer of the Black Sea. Appl. Sci. 11 (10), 4692. https://doi.org/10.3390/app11104692.

Viana, M., Hammingh, P., Colette, A., Querol, X., Degraeuwe, B., Vlieger, I. de, van Aardenne, J., 2014. Impact of maritime transport emissions on coastal air quality in Europe. Atmos. Environ. 90, 96–105. https://doi.org/10.1016/j.atmosenv.2014.03.046.

Wang, Y., Chen, H.-H., Tang, R., He, D., Lee, Z., Xue, H., Wells, M., Boss, E., Chai, F., 2022. Australian fire nourishes ocean phytoplankton bloom. Sci. Total Environ. 807, 150775. https://doi.org/10.1016/j.scitotenv.2021.150775.

Wang, L., Lei, X., Yuehua, G., Zhou, Y., Han, J.C., Huang, Y., Li, B., Mao, X.Z., Tang, Z., 2024. A novel method of identifying estuary high-nutrient zones for water quality management. Sci. Total Environ. 912, 169578. https://doi.org/10.1016/J.SCITOTENV.2023.169578.

Wang, X., Liu, H., Zhang, J., Fu, X., Chen, D., Zhang, W., Yi, W., Lv, Z., Zhang, Q., He, K., 2025. Global shipping emissions from 1970 to 2021: structural and spatial change driven by trade dynamics. One Earth 8 (4), 101243. https://doi.org/10.1016/J.ONEEAR.2025.101243.

Xu, L., Yu, H., Chen, Z., Du, W., Chen, N., Zhang, C., 2023. Monthly ocean primary productivity forecasting by joint use of seasonal climate prediction and temporal memory. Remote Sens. 15 (5). https://doi.org/10.3390/rs15051417.

Xuan, J.-L., Zhou, F., Huang, D.-J., Wei, H., Liu, C.-G., Xing, C.-X., 2011. Physical processes and their role on the spatial and temporal variability of the spring phytoplankton bloom in the central Yellow Sea. Acta Ecol. Sin. 31 (1), 61–70. https://doi.org/10.1016/J.CHNAES.2010.11.011.

Yu, H., Lu, Y., Fang, Z., Xu, L., 2025. How global container shipping emissions and marine primary production are related to: a geographically and temporally weighted analysis. Mar. Environ. Res. 209. https://doi.org/10.1016/j.marenvres.2025.107195.

Zhang, C., Shi, Z., Zhao, J., Zhang, Y., Yu, Y., Mu, Y., Yao, X., Feng, L., Zhang, F., Chen, Y., Liu, X., Shi, J., Gao, H., 2021. Impact of air emissions from shipping on marine phytoplankton growth. Sci. Total Environ. 769, 145488. https://doi.org/10.1016/J.SCITOTENV.2021.145488.